

## **Cobalt Adipate $\text{Co}(\text{C}_6\text{H}_8\text{O}_4)$ : Antiferromagnetic Structure, Unusual Thermal Expansion and Magnetoelastic Coupling**

### **Electronic Supplementary Information**

Paul J. Saines<sup>a\*</sup>, Phillip T. Barton<sup>b</sup>, Marek Jura<sup>c</sup>, Kevin S. Knight<sup>c</sup>  
and Anthony K. Cheetham<sup>d</sup>

<sup>a</sup> Department of Chemistry, University of Oxford, Inorganic Chemistry Laboratory, South Parks Road, Oxford, OX1 3QR, U.K.

<sup>b</sup> Materials Research Laboratory and Materials Department, University of California Santa Barbara, Santa Barbara, California 93106, USA.

<sup>c</sup> ISIS Facility, Rutherford Appleton Laboratory, Harwell Oxford, Didcot, OX11 0QX, U.K.

<sup>d</sup> Department of Materials Science and Metallurgy, University of Cambridge, Charles Babbage Road, Cambridge, CB3 0FS, U.K.

## Experimental

### Single Crystal Analysis

Absorption corrections of the single crystal X-ray measurements were carried out using the analytical methods implemented in CrysAlis Pro.<sup>12</sup> Refinements in SHELX-97<sup>14</sup> were carried out against  $|F^2|$  and the displacement parameters of all non-hydrogen atoms were refined anisotropically. The hydrogen atom positions were geometrically constrained using the AFIX commands in SHELX-97<sup>14</sup>, with thermal parameters of constrained to be 1.2 times the atoms on which they rode.

### Powder Neutron Diffraction

High quality patterns were recorded with a 2 g sample in a vanadium cylindrical can while the sample was placed in a square can to obtain shorter patterns for lattice parameter determination. In the Rietveld refinements carried out in GSAS,<sup>20</sup> the peaks shapes were modelled as convolutions of back-to-back exponentials with a pseudo-Voigt and the backgrounds were modelled using shifted Chebyschev polynomials. Distance restraints were applied, with a tolerance of 0.05 Å with values similar to those observed from single crystal structural analysis (1.95 Å, 1.50 Å and 1.25 Å for Co-O, C-C and C-O bonds), except for C-D bonds, which were constrained to 1.10 Å, typical of distances in the literature.<sup>6,22</sup>

## Supplementary Figures

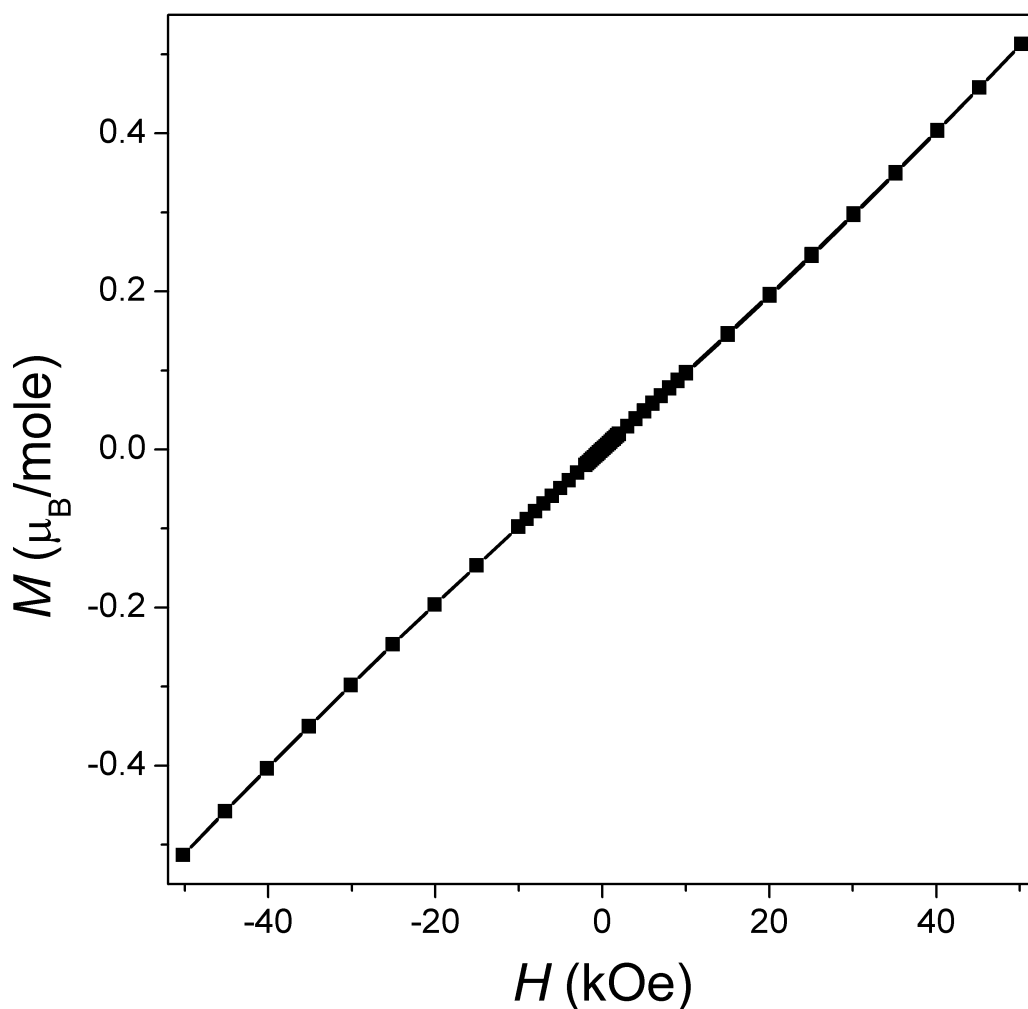


**Fig. S1:** Isothermal magnetisation measurements of  $\text{Co}(\text{C}_6\text{H}_8\text{O}_4)$  carried out at 12 K.

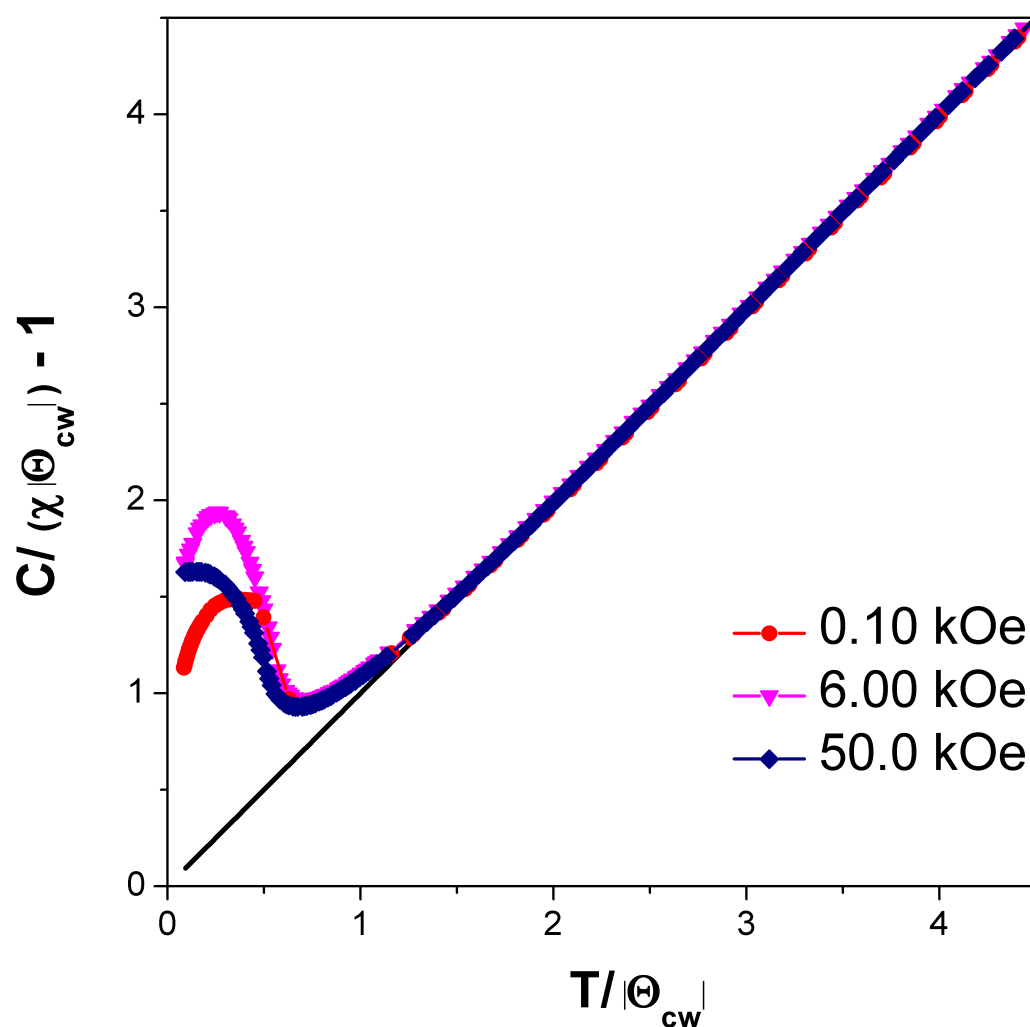


**Fig S2:** Scaled inversed susceptibility as a function of scaled temperature of  $\text{Co}(\text{C}_6\text{H}_8\text{O}_4)$  from 0.1, 6.00 and 50.0 kOe field cooled measurements.

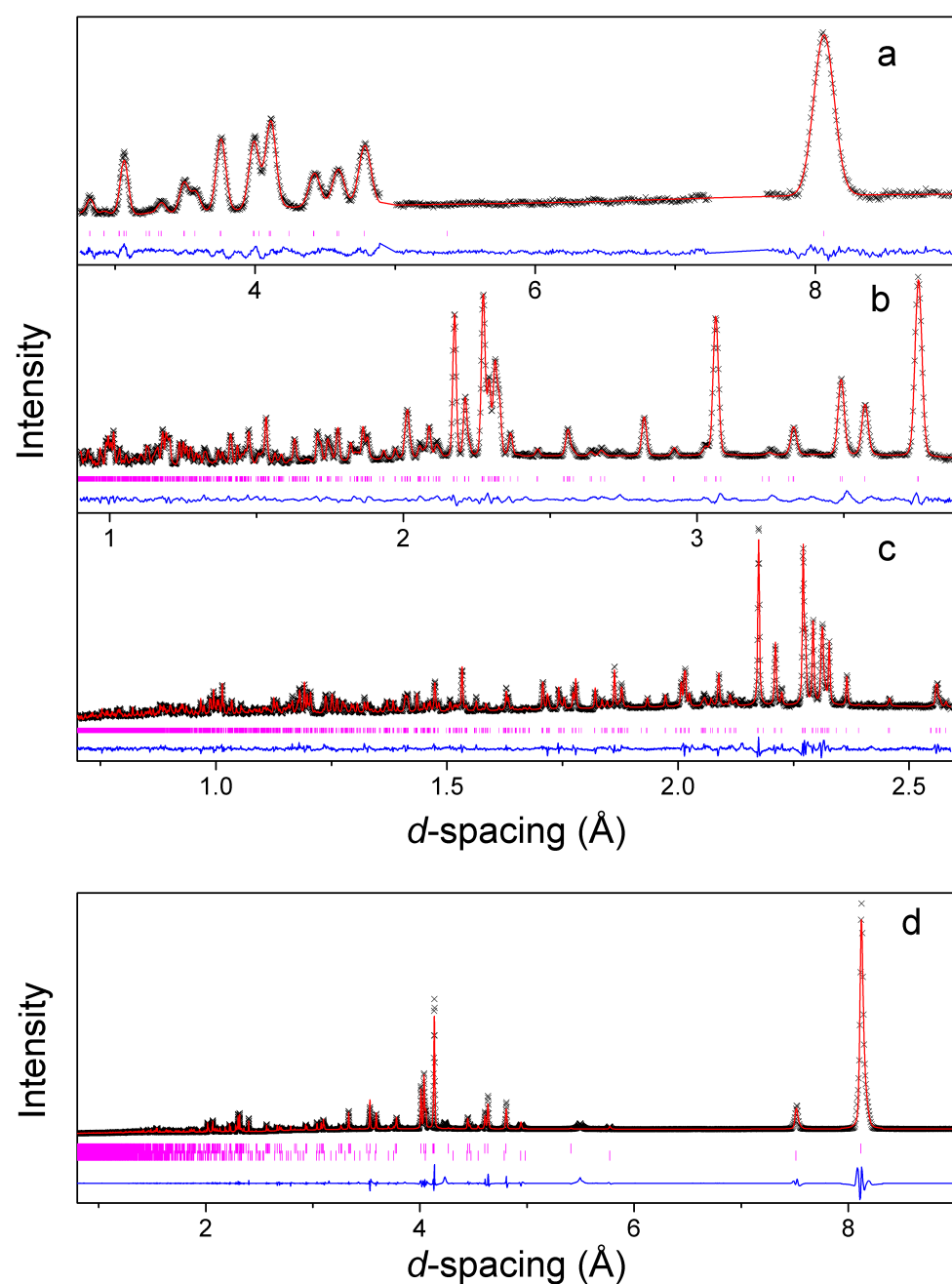


**Fig. S3:** Neutron (**a-c**) and synchrotron X-ray (**d**) powder diffraction patterns of  $\text{Co}(\text{C}_6\text{D}_8\text{O}_4)$  at 30 K and 300 K, respectively. The crosses, upper and lower continuous lines represent the observed intensities, calculated intensities and difference plots, respectively. The vertical markers represent the positions of the Bragg reflections, with the lower reflection markers in **d** representing the peaks caused by the known hydrated impurity. The neutron diffraction patterns **a-c** represent the low angle,  $90^\circ$  and back scattered banks, respectively. The omitted regions in the low angle pattern are the two most intense impurity peaks corresponding to the known hydrated impurity.

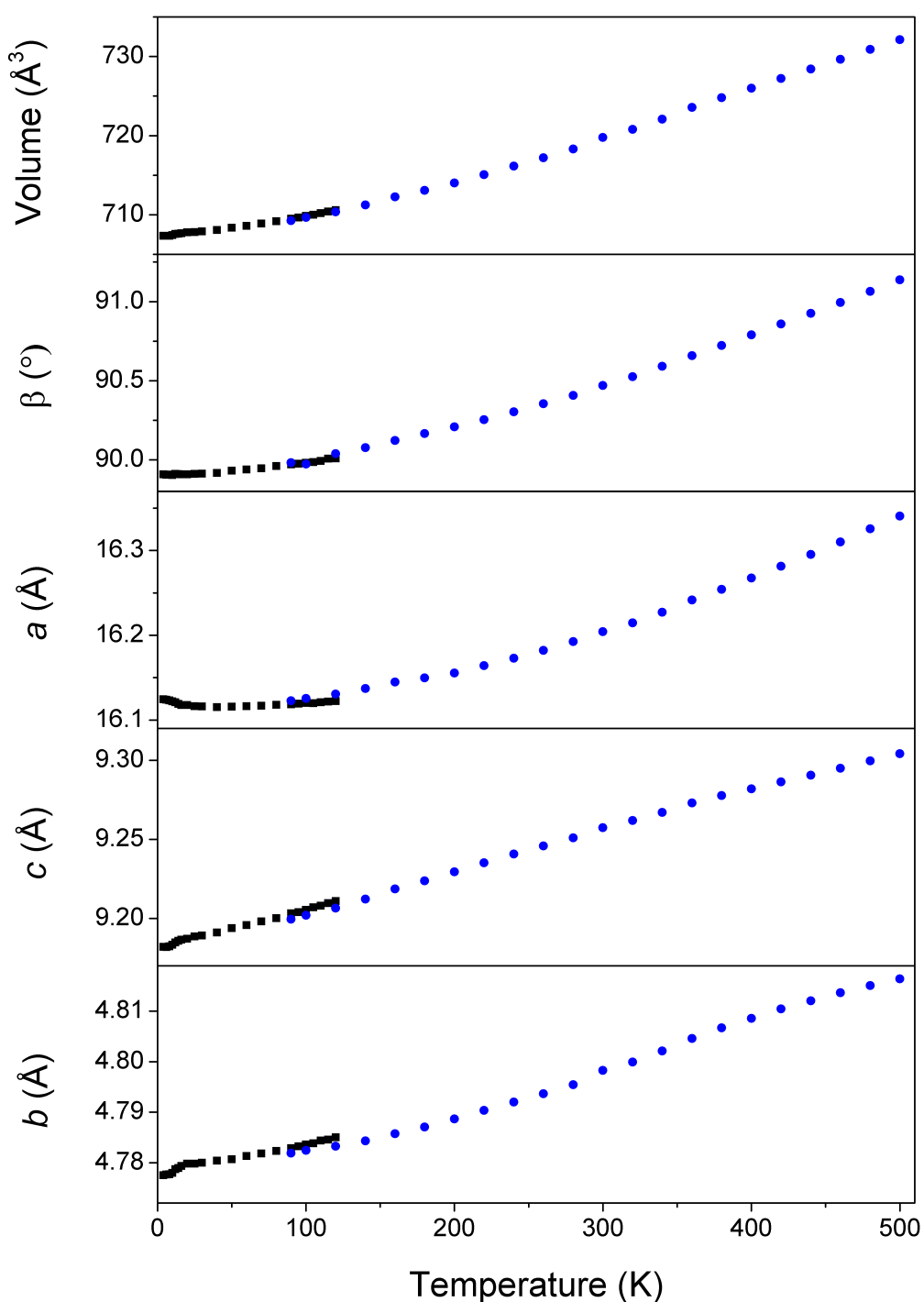


**Fig. S4:** Plots of lattice parameters versus temperature determined using neutron (square markers) and synchrotron X-ray (circular markers) powder diffraction.